

# Elongation of Planar Boron Clusters by Hydrogenation: Boron Analogues of Polyenes

Wei-Li Li, Constantin Romanescu, Tian Jian, and Lai-Sheng Wang\*

Department of Chemistry, Brown University, Providence, Rhode Island 02912, United States

**S** Supporting Information

**ABSTRACT:** Dihydrogenated boron clusters,  $H_2B_n^-$  ( $n = 7-12$ ), were produced and characterized using photoelectron spectroscopy and computational chemistry to have ladderlike structures terminated by a hydrogen atom on each end. The two rows of boron atoms in the dihydrides are bonded by delocalized three-, four-, or five-center  $\sigma$  and  $\pi$  bonds. The  $\pi$  bonding patterns in these boron nanoladders bear similarities to those in conjugated alkenes:  $H_2B_7^-$ ,  $H_2B_8^-$ , and  $H_2B_9^-$ , each with two  $\pi$  bonds, are similar to butadiene, while  $H_2B_{10}^{2-}$ ,  $H_2B_{11}^-$ , and  $H_2B_{12}^-$ , each with three  $\pi$  bonds, are analogous to 1,3,5-hexatriene. The boron cluster dihydrides can thus be considered as polyene analogues, or “polyboroenes”. Long polyboroenes with conjugated  $\pi$  bonds (analogous to polyacetylenes), which may form a new class of molecular wires, should exist.

Boron clusters have been found to possess two-dimensional (2D) planar structures in which all of the peripheral atoms are bonded by strong single B–B  $\sigma$  bonds and the inner boron atoms interact with the periphery via delocalized  $\sigma$  and  $\pi$  bonds for  $B_n$  clusters with  $n \geq 7$ .<sup>1–4</sup> The  $B_8$  and  $B_9$  clusters have perfect molecular wheel structures with one central atom,<sup>1</sup> while the central atom in  $B_7$  is slightly out of plane because the  $B_6$  ring is too small to host the B atom.<sup>5</sup> The delocalized  $\pi$  bonding is found to follow the Hückel rule for aromaticity, and the concept of planar boron clusters as hydrocarbon analogues has been proposed.<sup>1–3</sup> In fact, the  $\pi$  bonding in every planar boron cluster has been found to correspond to that of an aromatic hydrocarbon.<sup>6–8</sup> Negatively charged boron clusters are known to be planar at least up to  $B_{21}^-$ ,<sup>9</sup> whereas positively charged clusters start to be three-dimensional (3D) at  $B_{16}^+$ .<sup>10</sup> The 2D-to-3D transition occurs at  $B_{20}$  for neutral clusters.<sup>11</sup> The planar boron clusters are in stark contrast to bulk boron and borane compounds, where cage-like 3D structures dominate.<sup>12</sup> Hydrogenation of the planar boron clusters is expected to break the peripheral B–B  $\sigma$  bonds, leading to structural transformation. Partially hydrogenated boron clusters ( $B_nH_m$ ,  $n > m$ ) are expected to evolve into 3D borane-like structures as a function of  $m$ . This 2D-to-3D structural transition for  $B_{12}H_m^+$  clusters has been suggested to occur at  $B_{12}H_6^+$ .<sup>13,14</sup> An early theoretical study reported monohydrogenated boron cluster cations ( $B_nH^+$ ,  $n = 1-13$ ) to have structures similar to the bare  $B_n^+$  clusters.<sup>15</sup> The first dihydrogenated boron cluster studied computationally was  $H_2B_7^-$ ,<sup>16</sup> which was found to have a two-row elongated

structure with two terminal H atoms, quite different from the  $B_7^-$  global-minimum structure.<sup>5</sup> Its  $Au_2B_7^-$  auroanalogue was experimentally characterized and found to have the same structure as  $H_2B_7^-$ .<sup>17</sup>

Recently, a number of computational studies on hydrogenated boron clusters have been reported.<sup>18–25</sup> In addition to having interesting structures and bonding properties, partially hydrogenated boron clusters play important roles during dehydrogenation of boron hydride hydrogen-storage materials.<sup>20,21,26</sup> Here we report the first experimental observation and characterization of a series of dihydride boron clusters,  $H_2B_n^-$  ( $n = 7-12$ ), which were found to possess ladderlike elongated structures with two terminal H atoms. Chemical bonding analyses showed that the  $\pi$  bonding patterns in the boron cluster dihydrides are similar to those in conjugated alkenes, and thus, they can be viewed as hydrocarbon analogues, or “polyboroenes”. The polyboroenes and their auroanaluges ( $Au_2B_n$ ) with conjugated  $\pi$  bonding form a new class of molecular wires.

The experiments were carried out using a photoelectron spectroscopy apparatus equipped with a laser-vaporization supersonic cluster source.<sup>27</sup> The boron hydride cluster anions were produced by laser vaporization of an isotopically enriched  $^{11}B$  target with helium containing 5%  $D_2$  as the carrier gas. Clusters with various compositions ( $B_nD_m^-$ ) were formed in the plasma reactions between the laser-vaporized boron and  $D_2$ , which was used instead of  $H_2$  for better mass separation.<sup>28</sup> Under our experimental conditions, strong  $B_nD_m^-$  cluster signals were produced for  $n \geq 7$  and  $m = 1$  and 2. We found that the photoelectron spectra of  $D_2B_n^-$  were special, all with vibrational resolution, as shown in Figure 1. Spectra at higher photon energy (193 nm) are shown in Figure S1 in the Supporting Information, where comparisons with theoretical calculations are also shown. The vibrational resolution suggests that all of the  $D_2B_n^-$  clusters have relatively high symmetries and that there are no significant differences in geometry between the ground states of the anions and those of the neutrals. In particular, the photoelectron spectrum of  $D_2B_7^-$  (Figure 1A) is almost identical to that of  $Au_2B_7^-$ ,<sup>17</sup> indicating their similar structures and confirming the previously reported global-minimum structure of  $H_2B_7^-$ .<sup>16</sup>

We carried out theoretical calculations and found that the global minima of the  $H_2B_n^-$  clusters for  $n = 8-12$  (Figure 2) have ladder structures similar to that of  $H_2B_7^-$ .<sup>16,28</sup> For odd  $n$ , the two H atoms are in the cis position, whereas for even  $n$ , the

Received: June 18, 2012

Published: July 31, 2012

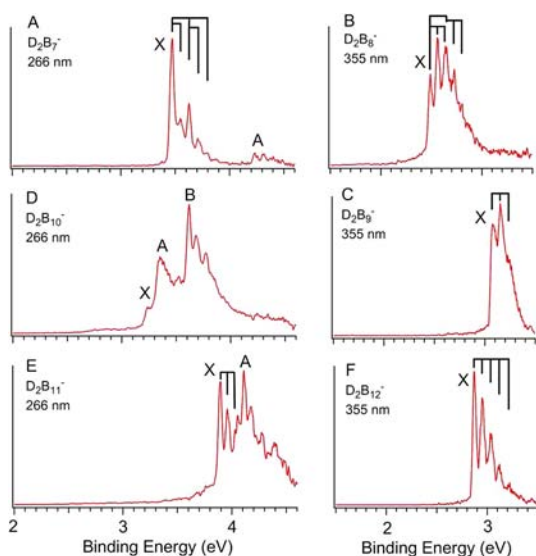


**Figure 1.** Photoelectron spectra of  $D_2B_n^-$  ( $n = 7-12$ ): (A)  $D_2B_7^-$  at 266 nm; (B)  $D_2B_8^-$  at 355 nm; (C)  $D_2B_9^-$  at 355 nm; (D)  $D_2B_{10}^-$  at 266 nm; (E)  $D_2B_{11}^-$  at 266 nm; (F)  $D_2B_{12}^-$  at 355 nm.

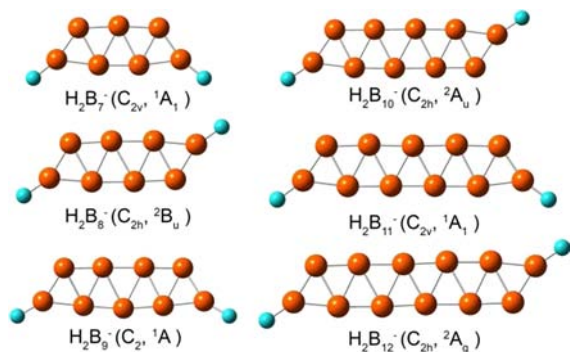


**Figure 2.** Optimized global-minimum structures for  $H_2B_n^-$  ( $n = 7-12$ ).

two H atoms are in the trans position. Our calculated low-lying structures for all of these species are given in the Figure S2. No low-lying isomers within 5 kcal/mol of the global-minimum ladder structures were found for  $n = 7,^{16} 8, 10$ , and 11. One or more low-lying isomers were found for  $n = 9$  and 12, consistent with the experimental observation that isomers were present in these cluster beams (Figure S1). The calculated adiabatic

detachment energies (ADEs) and vertical detachment energies (VDEs) for the global-minimum ladder structures are compared with the experimental data in Table 1. Good agreement between the calculated ADE/VDE and the experimental data is observed. The ADEs of  $D_2B_8^-$  and  $D_2B_{12}^-$  are low because their neutrals are closed-shell species with large energy gaps between their lowest unoccupied molecular orbitals (LUMOs) and highest occupied molecular orbitals (HOMOs), which were observed to be 1.63 and 1.47 eV for  $D_2B_8$  and  $D_2B_{12}$ , respectively (Figure S1), suggesting that they are highly stable neutral species. The neutral  $D_2B_{10}$  ladder structure has a nearly degenerate closed-shell singlet state and a triplet state with two unpaired electrons, in agreement with the observed high ADE of  $D_2B_{10}^-$  and the small energy gap between the first and second detachment transitions (Figure 1D). This observation suggests that  $D_2B_{10}^{2-}$  should be a stable closed-shell species, which will be used in the chemical bonding analysis below. All of the odd-sized  $D_2B_n^-$  clusters have closed-shell electronic structures, giving rise to high ADEs, except for  $D_2B_9^-$ . The relatively low ADE of  $D_2B_9^-$  suggests that its HOMO is unstable, in agreement with the large observed energy gap between the first and second detachment transitions (Figure S1). In fact, the global-minimum structure of  $D_2B_9^-$  is not perfectly planar, and the  $B_9$  ladder framework has a slight out-of-plane twist, giving rise to  $C_2$  symmetry (Figure 2). The broader vibrational line width in the photoelectron spectrum of  $D_2B_9^-$  (Figure 1C) is consistent with the excitation of a low-frequency vibrational mode, because neutral  $D_2B_9$  is planar with  $C_{2v}$  symmetry (Figure S3) and has a very low frequency bending mode. These observations suggest that  $D_2B_9^+$  should be a more stable closed-shell planar species, which was confirmed by our calculations. The simulated spectra using the calculated VDEs for the global-minimum ladder structures are compared with the 193 nm photoelectron spectra in Figure S1 for all of the dihydrides. The overall agreement between the theoretical and experimental data is excellent, lending considerable credence to the identified ladderlike structures for the boron cluster dihydride anions.

The resolved vibrational information for the ground-state transition provides additional support for the ladder structures of the dihydride clusters. The observed vibrational frequencies are compared with the calculated frequencies for the  $D_2B_n$  ground states in Table 1. The calculated vibrational frequencies for the totally symmetric modes of the neutrals and the corresponding normal mode assignments are given in Figure S4. In each case, the active normal modes are consistent with

**Table 1.** Observed and Calculated ADEs, VDEs, and Vibrational Frequencies for the Ground-State Photodetachment Transitions of  $D_2B_n^-$  ( $n = 7-12$ )

	experimental <sup>a</sup>		calculated					
	ADE (eV)	VDE (eV)	vib. freq. (cm <sup>-1</sup> )		ADE (eV)	VDE (eV)	vib. freq. (cm <sup>-1</sup> )	
			$\nu_1$	$\nu_2$			$\nu_1$	$\nu_2$
$D_2B_7^-$ ( $^1A_1, C_{2v}$ ) <sup>b</sup>	3.49(3)	3.49(3)	1250(40)	620(40)	3.35	3.47	1323	609
$D_2B_8^-$ ( $^2B_u, C_{2h}$ )	2.49(3)	2.56(3)	1230(50)	550(40)	2.60	2.75	1232	516
$D_2B_9^-$ ( $^1A, C_2$ )	3.07(3)	3.15(3)		630(40)	2.92	3.04		636
$D_2B_{10}^-$ ( $^2A_u, C_{2h}$ )	3.24(3)	3.35(4)			3.44	3.57		
$D_2B_{11}^-$ ( $^1A_1, C_{2v}$ )	3.89(3)	3.89(3)		550(40)	3.79	3.91		581
$D_2B_{12}^-$ ( $^2A_g, C_{2h}$ )	2.87(3)	2.87(3)		680(40)	2.98	3.04		680

<sup>a</sup>Numbers in parentheses are the uncertainties in the last digits. <sup>b</sup>The photoelectron spectra of  $H_2B_7^-$  were also measured. The measured and calculated ADEs and VDEs were the same as those of  $D_2B_7^-$ . The corresponding measured vibrational frequencies for the ground state of  $H_2B_7^-$  were  $\nu_1 = 1350(40)$  cm<sup>-1</sup> and  $\nu_2 = 720(40)$  cm<sup>-1</sup>, while the calculated values were  $\nu_1 = 1335$  cm<sup>-1</sup> and  $\nu_2 = 681$  cm<sup>-1</sup>.

the nature of the HOMO from which the electron is detached (Figure S5) and the differences in the ground-state geometries of the anion and the neutral (Figure S3).

We performed chemical bonding analyses of the boron cluster dihydrides using the adaptive natural density partitioning (AdNDP) method.<sup>29,30</sup> AdNDP is based on the concept that electron pairs are the main elements of the chemical bonds. It represents the molecular electronic structure in terms of  $n$ -center two-electron ( $nc-2e$ ) bonds, recovering the familiar lone pairs ( $1c-2e$ ) and localized  $2c-2e$  bonds or delocalized  $nc-2e$  bonds ( $3 \leq n \leq$  total number of atoms in the system). Figure 3 shows the AdNDP results for  $H_2B_7^-$ ,  $H_2B_8$ ,  $H_2B_9^-$ ,

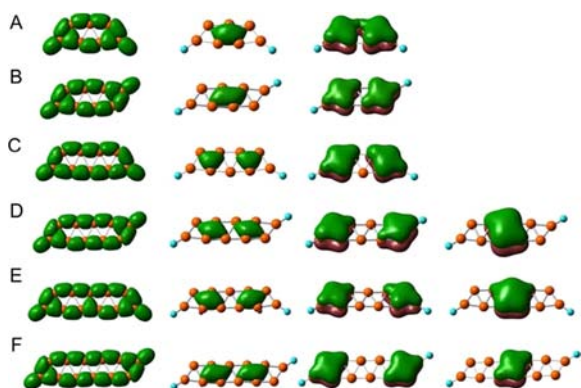


**Figure 3.** Chemical bonding analyses using the AdNDP method: (A)  $H_2B_7^-$ ; (B)  $H_2B_8$ ; (C)  $H_2B_9^-$ ; (D)  $H_2B_{10}^{2-}$ ; (E)  $H_2B_{11}^-$ ; (F)  $H_2B_{12}$ .

$H_2B_{10}^{2-}$ ,  $H_2B_{11}^-$ , and  $H_2B_{12}$  calculated using the Multiwfn program.<sup>31</sup> These charge states were chosen because the AdNDP method can handle only closed-shell systems.<sup>29-31</sup> The B–H bonds and the peripheral B–B bonds are described mainly as  $2c-2e$  localized  $\sigma$  bonds, except for a few cases where some  $3c-2e$  bonding character is also seen. The peripheral B–B bonding is similar to that observed in all of the planar boron clusters.<sup>1-9</sup> The two rows of boron atoms in the ladder structures are bonded via multicenter  $\sigma$  and  $\pi$  bonds.  $H_2B_7^-$ ,  $H_2B_8$ , and  $H_2B_9^-$ , each with two  $4c-2e$   $\pi$  bonds (four  $\pi$  electrons), can be considered to be antiaromatic according to the Hückel  $4n$  rule. This bonding property in  $H_2B_7^-$  (or its auroanalogue,  $Au_2B_7^-$ ) has been compared with that in the prototypical antiaromatic cyclobutadiene.<sup>16,17</sup>  $H_2B_{10}^{2-}$ ,  $H_2B_{11}^-$ , and  $H_2B_{12}$ , each with three delocalized  $\pi$  bonds (six  $\pi$  electrons), can be considered to be aromatic according to the Hückel  $4n + 2$  rule. However, the elongated shapes of  $H_2B_{10}^{2-}$ ,  $H_2B_{11}^-$ , and  $H_2B_{12}$  are not consistent with  $\pi$  aromaticity, which usually leads to more circular structures in boron clusters<sup>1-9</sup> and the recently discovered transition-metal-centered boron clusters.<sup>32-34</sup>

We noticed that the  $\pi$  bonds in the dihydrides are delocalized only over parts of the boron ladder frameworks, and they can be viewed as  $\pi$  bonds between two pairs of boron atoms, reminiscent of the  $\pi$  bonds in conjugated alkenes. The two  $\pi$  orbitals in  $H_2B_7^-$ ,  $H_2B_8$ , and  $H_2B_9^-$  are compared with those of butadiene in Figure 4A, and the three  $\pi$  orbitals of  $H_2B_{10}^{2-}$ ,  $H_2B_{11}^-$ , and  $H_2B_{12}$  are compared with those of 1,3,5-hexatriene in Figure 4B. This similarity in  $\pi$  bonding suggests that the boron cluster dihydrides should be considered more appropriately as analogues of polyenes and thus may be called “polyboroenes”. In particular, each pair of boron atoms in  $H_2B_8$  and  $H_2B_{12}$  can be viewed as contributing one  $\pi$  electron

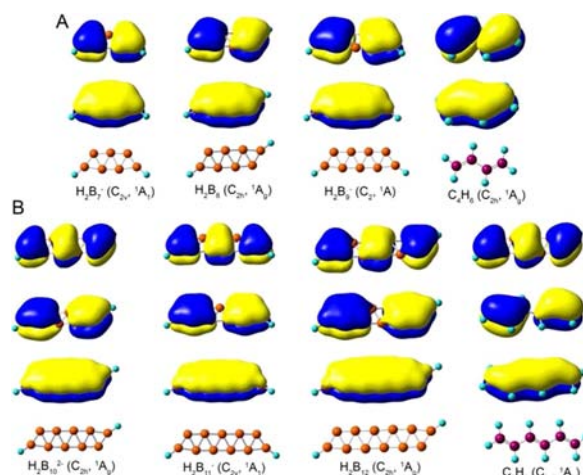


**Figure 4.** Comparison of the  $\pi$  molecular orbitals of the boron cluster dihydrides with those of conjugated alkenes: (A)  $\pi$  orbitals of  $H_2B_7^-$ ,  $H_2B_8$ ,  $H_2B_9^-$ , and butadiene ( $C_4H_6$ ); (B)  $\pi$  orbitals of  $H_2B_{10}^{2-}$ ,  $H_2B_{11}^-$ ,  $H_2B_{12}$ , and 1,3,5-hexatriene ( $C_6H_8$ ).

to form a  $4c-2e$   $\pi$  bond with the adjacent  $B_2$  pair in each  $B_4$  unit, while there is a delocalized  $4c-2e$   $\sigma$  bond between two  $B_4$  units in  $H_2B_8$  and  $H_2B_{12}$ . We think that it is this perfect alternating  $4c-2e$   $\pi$  and  $4c-2e$   $\sigma$  bonding pattern in  $H_2B_8$  and  $H_2B_{12}$  that contributes to their high electronic stability and the large HOMO–LUMO gap in these two dihydrides. Similar  $\pi$  and  $\sigma$  bonding patterns are expected to exist in all of the  $H(B_4)_xH$  dihydrides ( $x = 1, 2, 3, \dots$ ), which should form a series similar to polyacetylenes,  $H(CH=CH)_xH$ .

On the bases of the stable closed-shell  $H_2B_7^-$ ,  $H_2B_{10}^{2-}$ , and  $H_2B_9^+$  species, there should also exist three similar series of charged dihydride polyboroenes,  $[H_2(B_4)_xB_3]^-$ ,  $[H_2(B_4)_xB_2]^{2-}$ , and  $[H_2(B_4)_xB]^+$ . Since Au has been found to behave like a hydrogen atom to form covalent bonds,<sup>35,36</sup> such as those found in  $Au_2B_7^-$ ,<sup>17</sup> it is expected that the auroanalogue (or auropolyboroenes)  $Au_2(B_4)_x$ ,  $[Au_2(B_4)_xB_3]^-$ ,  $[Au_2(B_4)_xB_2]^{2-}$ , and  $[Au_2(B_4)_xB]^+$  should also be highly stable molecular species. The polyboroenes or auropolyboroenes may be synthesized in the bulk or deposited on surfaces to give a new family of molecular wires.

**Photoelectron spectroscopy.** The experiments were carried out using a photoelectron spectroscopy apparatus equipped with a laser-vaporization supersonic cluster source.<sup>27</sup> The boron hydride cluster anions were produced by laser vaporization of an isotopically enriched  $^{11}B$  target (96%) with helium containing 5%  $D_2$  as the carrier gas. Clusters with various compositions ( $B_nD_m^-$ ) were formed in the plasma reactions between the laser-vaporized boron and  $D_2$ , which was used instead of  $H_2$  for better mass separation.<sup>28</sup> The nascent clusters were entrained in the helium carrier gas and underwent a supersonic expansion. Negatively charged clusters were extracted from the cluster beam and subjected to a time-of-flight mass analysis. The clusters of interest were mass-selected and decelerated before being photodetached by a laser beam. In the current study, three photon energies were used: 355 nm (3.496 eV) and 266 nm (4.661 eV) from an Nd:YAG laser and 193 nm (6.424 eV) from an ArF excimer laser. Photoemitted electrons were analyzed by a magnetic-bottle electron analyzer with a kinetic energy resolution of  $\Delta E_k/E_k = 2.5\%$  (i.e., 25 meV for 1 eV electrons). The apparatus was calibrated using the known photoelectron spectrum of  $Bi^-$ .

**Computational methods.** The search for the global minima of  $H_2B_n^-$  ( $8 \leq n \leq 12$ ) was performed using the simulated annealing algorithm.<sup>37</sup> Up to 2000 structures were initially optimized using the PBE0 hybrid density functional<sup>38–40</sup> and the 3-21G basis set<sup>41</sup> as implemented in the Gaussian 09 program.<sup>42</sup> The low-energy structures revealed by the initial screening ( $\Delta E < 50$  kcal/mol) were further reoptimized at the PBE0/6-311++G(d,p) level of theory.<sup>43–45</sup> The theoretical ADEs and VDEs for the global-minimum structures and competing low-lying isomers were calculated at the same level of theory. For the vibrational assignments of the experimental spectra, frequency calculations were performed for the corresponding  $D_2B_n^{-/0}$  ( $7 \leq n \leq 12$ ) species. Chemical bonding analyses of the clusters were performed using the AdNDP method<sup>29,30</sup> as implemented in the Multiwfn 2.4 program.<sup>31</sup> GaussView 4.1.2 was used for MO visualization.

## ■ ASSOCIATED CONTENT

### ■ Supporting Information

Photoelectron spectra at 193 nm, comparisons with theoretical calculations, all of the low-lying isomers, comparison of anion and neutral ladder structures, calculated vibrational frequencies for the totally symmetric modes and the observed normal modes, all of the MOs for each cluster, and complete ref 42. This material is available free of charge via the Internet at <http://pubs.acs.org>.

## ■ AUTHOR INFORMATION

### Corresponding Author

lai-sheng\_wang@brown.edu

### Notes

The authors declare no competing financial interest.

## ■ ACKNOWLEDGMENTS

This research was supported by the NSF (DMR-0904034).

## ■ REFERENCES

- Zhai, H. J.; Alexandrova, A. N.; Birch, K. A.; Boldyrev, A. I.; Wang, L. S. *Angew. Chem., Int. Ed.* **2003**, *42*, 6004.
- Zhai, H. J.; Kiran, B.; Li, J.; Wang, L. S. *Nat. Mater.* **2003**, *2*, 827.
- Alexandrova, A. N.; Boldyrev, A. I.; Zhai, H. J.; Wang, L. S. *Coord. Chem. Rev.* **2006**, *250*, 2811.
- Zubarev, D. Y.; Boldyrev, A. I. *J. Comput. Chem.* **2007**, *28*, 251.
- Alexandrova, A. N.; Boldyrev, A. I.; Zhai, H. J.; Wang, L. S. *J. Phys. Chem. A* **2004**, *108*, 3509.
- Sergeeva, A. P.; Zubarev, D. Y.; Zhai, H. J.; Boldyrev, A. I.; Wang, L. S. *J. Am. Chem. Soc.* **2008**, *130*, 7244.
- Huang, W.; Sergeeva, A. P.; Zhai, H. J.; Averkiev, B. B.; Wang, L. S.; Boldyrev, A. I. *Nat. Chem.* **2010**, *2*, 202.
- Sergeeva, A. P.; Averkiev, B. B.; Zhai, H. J.; Boldyrev, A. I.; Wang, L. S. *J. Chem. Phys.* **2011**, *134*, No. 224304.
- Piazza, Z. A.; Li, W. L.; Romanescu, C.; Sergeeva, A. P.; Wang, L. S.; Boldyrev, A. I. *J. Chem. Phys.* **2012**, *136*, No. 104310.
- Oger, E.; Crawford, N. R. M.; Keltling, R.; Weis, P.; Kappes, M. M.; Ahlrichs, R. *Angew. Chem., Int. Ed.* **2007**, *46*, 8503.
- Kiran, B.; Bulusu, S.; Zhai, H. J.; Yoo, S.; Zeng, X. C.; Wang, L. S. *Proc. Natl. Acad. Sci. U.S.A.* **2005**, *102*, 961.
- Greenwood, N. N.; Earnshaw, A. *Chemistry of the Elements*; Butterworth-Heinemann: London, 1997.
- Ohishi, Y.; Kimura, K.; Yamaguchi, M.; Uchida, N.; Kanayama, T. *J. Chem. Phys.* **2008**, *128*, No. 124304.
- Bai, H.; Li, S. D. *J. Cluster Sci.* **2011**, *22*, 525.
- Ricca, A.; Bauschlicher, C. W. *J. Chem. Phys.* **1997**, *106*, 2317.
- Alexandrova, A. N.; Koyle, E.; Boldyrev, A. I. *J. Mol. Model.* **2006**, *12*, 569.
- Zhai, H. J.; Wang, L. S.; Zubarev, D. Y.; Boldyrev, A. I. *J. Phys. Chem. A* **2006**, *110*, 1689.
- Ohishi, Y.; Kimura, K.; Yamaguchi, M.; Uchida, N.; Kanayama, T. *J. Chem. Phys.* **2010**, *133*, No. 074305.
- Szwacki, N. G.; Weber, V.; Tymczak, C. J. *Nanoscale Res. Lett.* **2009**, *4*, 1085.
- Olson, J. K.; Boldyrev, A. I. *Inorg. Chem.* **2009**, *48*, 10060.
- Olson, J. K.; Boldyrev, A. I. *J. Chem. Phys.* **2011**, *379*, 1.
- Olson, J. K.; Boldyrev, A. I. *J. Chem. Phys. Lett.* **2011**, *517*, 62.
- Galeev, T. R.; Chen, Q.; Guo, J. C.; Bai, H.; Miao, C. Q.; Lu, H. C.; Sergeeva, A. P.; Li, S. D.; Boldyrev, A. I. *J. Phys. Chem. Chem. Phys.* **2011**, *13*, 11575.
- Chen, Q.; Bai, H.; Guo, J. C.; Miao, C. Q.; Li, S. D. *J. Phys. Chem. Chem. Phys.* **2011**, *13*, 20620.
- Chen, Q.; Li, S. D. *J. Cluster Sci.* **2011**, *22*, 513.
- Nguyen, V. S.; Matus, M. H.; Nguyen, M. T.; Dixon, D. A. *J. Phys. Chem. C* **2007**, *111*, 9603.
- Wang, L. S.; Cheng, H. S.; Fan, J. W. *J. Chem. Phys.* **1995**, *102*, 9480.
- Calculations for both  $H_2B_n^-$  and  $D_2B_n^-$  were performed. Except the vibrational frequencies, the structures and electron binding energies for the hydrogenated and deuterated species were identical.
- Zubarev, D. Y.; Boldyrev, A. I. *J. Phys. Chem. Chem. Phys.* **2008**, *10*, 5207.
- Zubarev, D. Y.; Boldyrev, A. I. *J. Org. Chem.* **2008**, *73*, 9251.
- Lu, T.; Chen, F. W. *J. Comput. Chem.* **2012**, *33*, 580.
- Romanescu, C.; Galeev, T. R.; Li, W. L.; Boldyrev, A. I.; Wang, L. S. *Angew. Chem., Int. Ed.* **2011**, *50*, 9334.
- Li, W. L.; Romanescu, C.; Galeev, T. R.; Piazza, Z. A.; Boldyrev, A. I.; Wang, L. S. *J. Am. Chem. Soc.* **2012**, *134*, 165.
- Galeev, T. R.; Romanescu, C.; Li, W. L.; Wang, L. S.; Boldyrev, A. I. *Angew. Chem., Int. Ed.* **2012**, *51*, 2101.
- Kiran, B.; Li, X.; Zhai, H. J.; Cui, L. F.; Wang, L. S. *Angew. Chem., Int. Ed.* **2004**, *43*, 2125.
- Wang, L. S. *J. Phys. Chem. Chem. Phys.* **2010**, *12*, 8694.
- Kirkpatrick, S.; Gelatt, C. D. J.; Vecchi, M. P. *Science* **1983**, *220*, 671.
- Perdew, J. P.; Burke, K.; Ernzerhof, M. *Phys. Rev. Lett.* **1996**, *77*, 3865.
- Perdew, J. P.; Burke, K.; Ernzerhof, M. *Phys. Rev. Lett.* **1997**, *78*, 1396.
- Adamo, C.; Barone, V. *J. Chem. Phys.* **1999**, *110*, 6158.
- Binkley, J. S.; Pople, J. A.; Hehre, W. J. *J. Am. Chem. Soc.* **1980**, *102*, 939.
- Frisch, M. J.; et al. *Gaussian 09*; Gaussian, Inc.: Wallingford, CT, 2009.
- Gordon, M. S.; Binkley, J. S.; Pople, J. A.; Pietro, W. J.; Hehre, W. J. *J. Am. Chem. Soc.* **1982**, *104*, 2797.
- Pietro, W. J.; Francl, M. M.; Hehre, W. J.; Defrees, D. J.; Pople, J. A.; Binkley, J. S. *J. Am. Chem. Soc.* **1982**, *104*, 5039.
- Clark, T.; Chandrasekhar, J.; Spitznagel, G. W.; Schleyer, P. v. R. *J. Comput. Chem.* **1983**, *4*, 294.
- Dennington, R.; Keith, T.; Millam, J. *GaussView*, version 4.1.2; Semichem, Inc.: Shawnee Mission, KS, 2007.